

---

## Construction of permittivity functions for high-explosives using density functional theory

---

Daniel Finkenstadt\*

Physics Department,  
US Naval Academy,  
Annapolis, Maryland 21402, USA  
E-mail: finkenst@usna.edu  
\*Corresponding author

Samuel George Lambrakos, Noam Bernstein,  
Verne L. Jacobs and Lulu Huang

US Naval Research Laboratory,  
4555 Overlook Avenue, SW,  
Washington, District of Columbia 20375, USA  
E-mail: lambrakos@anvil.nrl.navy.mil  
E-mail: noam.bernstein@nrl.navy.mil  
E-mail: jacobs@dave.nrl.navy.mil  
E-mail: huang@nrl.navy.mil

Lou Massa

Hunter College,  
City University of New York,  
695 Park Avenue, New York, New York 10065, USA  
E-mail: lmassa@hunter.cuny.edu

Andrew Shabaev

School of Physics, Astronomy, and Computational Sciences,  
George Mason University,  
4400 University Drive, Fairfax, Virginia 22030, USA  
E-mail: ashabaev@gmu.edu

**Abstract:** We review a framework for the prediction of explosive molecular spectra, namely, for the common explosives found in improvised explosive devices, e.g.,  $\beta$ -HMX. Through the use of excitation by incident electromagnetic waves in the THz frequency range, molecular signatures of these explosives may be detected, identified and perhaps neutralised remotely. A central component of this framework is an S-matrix representation of multilayered composite materials. The individual molecules are first simulated using first-principles density functional theory (DFT). An effective electric permittivity function is then constructed, which yields reflectivity and transmissivity functions of frequency and of angle of incident radiation. The input for this component would be a parameterised analytic-function

representation of the electric permittivity as a function of frequency, which is provided by another component model of the framework. The permittivity function is constructed by fitting response spectra calculated using DFT, and parameters are adjusted according to additional information available, e.g., from experimentally-measured spectra or theory-based assumptions concerning spectral features. Finally, a prototype simulation is described that considers the response characteristics for THz excitation of typical high explosives.

**Keywords:** terahertz spectroscopy; high explosives; density functional theory; improvised explosive devices.

**Reference** to this paper should be made as follows: Finkenstadt, D., Lambrakos, S.G., Bernstein, N., Jacobs, V.L. and Huang, L., Massa, L. and Shabaev, A. (2012) 'Construction of permittivity functions for high-explosives using density functional theory', *Int. J. Intelligent Defence Support Systems*, Vol. 5, No. 1, pp.24–43.

**Biographical notes:** Daniel Finkenstadt is an Assistant Professor of Physics at the US Naval Academy in Annapolis, MD, where he has taught physics since 2008. From 2005–2008, he held an appointment as National Research Council Postdoctoral Fellow, researching the electronic-structure of graphene and other materials under the supervision of Dr. Michael Mehl at the US Naval Research Laboratory (NRL). In 2005, he obtained his PhD from the University of Illinois, Urbana-Champaign, on the topic of density-functional theory applied to disordered materials under Professor Duane D. Johnson. He is currently researching titanium alloys as structural materials, improvements to density functional theory, relativistic corrections for Actinide chemistry, equations-of-state for warm, dense matter, THz spectra of explosives and IED detection. He has authored 18 publications on materials physics. He has had visiting appointments at NRL, the University of Illinois and Lawrence Livermore National Laboratory.

Samuel George Lambrakos has been at NRL for 28 years. He is currently a Research Physicist in the Center for Computational Materials Science in the Materials Science and Technology Division. His area of expertise is computational physics, which has included modelling of physical systems at the atomic level (molecular dynamics and quantum mechanics based simulations), as well as macroscopic phenomena (fluid dynamics and inverse modelling based simulations).

Noam Bernstein is a Research Physicist at NRL's Center for Computational Materials Science, where he leads a research programme on simulations of mechanical and structural properties of materials. He has been in the forefront of the development of coupled multiscale simulations since joining NRL, with experience in methods that combine various atomistic descriptions, including density functional theory and interatomic potentials, as well as continuum elasticity. He has applied these methods to the study of fracture and liquids. In addition, he has studied structural and mechanical properties of many other solid and molecular systems, with recent work on amorphous silicon and synthetic structural polypeptides.

Verne L. Jacobs became a Research Physicist at NRL in 1977. Before that, he worked for Science Applications, Inc. and held a Weizmann Fellowship at the Weizmann Institute of Science, in Israel. In 1968, at Berkeley, he conducted his PhD research in solid-state theory under the supervision of Professor Charles Kittel and in atomic theory under the supervision of Professors Charles L. Schwartz and Kenneth M. Watson. He has been an author of approximately 60

publications on atomic physics and an organiser of five scientific workshops and conferences. In 1989, he was an invited participant in the programme on ‘Atoms and ions in strongly coupled plasmas’, at the Institute for Theoretical Physics, University of California, Santa Barbara, California. In 1985, he was elected to Fellowship in the American Physical Society. His current interests include atomic radiative processes in electron-ion beam interactions and in high-temperature plasmas, with particular emphasis on dielectronic recombination and other processes involving autoionisation resonances.

Lulu Huang is a Scientist at the Center for Computational Materials Science at NRL. She obtained her PhD in Analytical Chemistry from the City University of New York in 1993, and was a Postdoctoral Fellow there for two years. Since 1995, she spent most of her career working with Nobel Laureate Dr. Jerome Karle, first for GEO-Center Inc, and later for the Laboratory for the Structure of Matter at NRL. She continued to serve at NRL after Dr. Karle’s retirement in 2009. She is one of the creators of the Kernel Energy Method, which solves the computational difficulty associated with ab-initio calculations for large size bio-molecules. She has developed a new way of discovering better explosive molecules that reduces the cost of testing, improves safety, and expands the possibility of discovering many new and superior explosive molecules.

Lou Massa is a Professor of Chemistry and Physics at Hunter College and the Graduate School of the City University of New York. He obtained his PhD in Chemical Physics at Georgetown University in 1966. He held a postdoctoral appointment at Brookhaven National Lab from 1966–1969, after which he transferred to Hunter College. He has had visiting appointments at the IBM Watson Research Lab, the University of North Carolina at Chapel Hill, the University of Bordeaux, the University of London, NRL, the Naval Surface Warfare Center, and Grumman Aerospace. He has been interested in subjects related to quantum crystallography, Boron fullerenes, density functional theory, transition state for formation of the peptide bond in the ribosome and scaling laws of infrared radiation.

Andrew Shabaev is a Research Assistant Professor at George Mason University. His research interests include electronic, magnetic and vibrational properties of bulk materials and nanometers size structures and their response in electromagnetic fields; pump-probe techniques for optical read-out and control of the ground and excited states of nanostructures; and applied projects in the field of computational materials science.

---

## 1 Introduction

Terahertz spectroscopy has been investigated for the past decade as a means for explosives detection. Although barriers like water vapour and clothing can attenuate some amount of the THz radiation meant to probe the explosives, it is hoped that some portion of the absorption spectra signal could properly indicate that an explosive is present.

Recently, it has been questioned whether this method is even possible at all (Kemp, 2011). Although electromagnetic radiation in the 30 GHz – 3 THz range can penetrate many common materials and at the same time probe the chemical structure of several explosives, the question remains: is there any reason to believe that a sensitive device or technician could distinguish HMX from even milk chocolate? This example is no mere

hyperbole; it turns out that the spectra of these two substances are quite similar. How is it possible, then, to distinguish two spectroscopically-similar materials that are embedded within (say) a layered matrix of one another? The question boils down to the non-uniqueness of various signatures associated with the dielectric response of composite materials.

Here we address how one would setup a framework for a range of detector configurations that could address the issue of non-uniqueness. The model representing the central component of this framework, to which the outputs of all the other components are inputs, is that of an S-matrix representation of multilayered composites. Each layer of the system is characterised by an average thickness and effective electric permittivity function (Jaruwatanadilok et al., 2006). The outputs are the reflectivity and transmissivity as a function of frequency and angle of the incident electromagnetic wave. Another component, which provides input to the S-matrix, is that of a parameterised analytic-function representing the electric permittivity as a function of frequency for each layer. This function is constructed by fitting response spectra calculated using density functional theory (DFT) (Hohenberg and Kohn, 1964; Kohn and Sham, 1965; Jones and Gunnarson, 1989). Parameters other than those provided by DFT are adjusted according to additional information that may be available, e.g., from experimentally-measured spectra or theory. The two-component model, which provides input to the parameterised permittivity function, represents the molecular structure of the explosive, as understood from a detailed DFT calculation and any other parametric representation, e.g., based on experimental measurements.

The majority of what follows is a review of work presented in various publications (Shabaev et al., 2010, 2011a, 2011b, 2011c), but an updated treatment is given to the general simulation framework, namely, a prototype simulation is described that considers response characteristics for THz excitation of the high explosive  $\beta$ -HMX. This prototype simulation includes a procedure for calculating response spectra using DFT as input to the S-matrix model. For this purpose, the DFT software NRLMOL was adopted (Pederson and Jackson, 1990; Jackson and Pederson, 1990; Briley et al., 1998; Porezag and Pederson, 1996; Porezag and Pederson, 1999; Pederson et al., 2000; Jackson et al., 1997).

It is important to note that the numerical-simulation framework to be presented is structured for two major purposes, which are complementary. One purpose, which relates directly to practical application, is the simulation of various possible scenarios for the detection of IEDs corresponding to the presence of various types of intermediate material layers between the explosive and detector. The other purpose, which relates indirectly to practical application, but is yet extremely important for the interpretation and design of detection strategies, is the quantitative analysis of absolute bounds, or rather, the inherent limitation on levels of detection associated with various types of detection strategies. It is this final aspect, related to the recent work in Kemp (2011) on the distinguishability of spectra, that we feel is best addressed by the S-matrix formalism of composite materials.

## 2 Literature review – DFT-calculated THz spectra for explosives

Over the past two years, the present authors have built a database of *ab initio* DFT results for THz spectra of the common explosive molecules. These are meant for use in a larger

project on calculating the dielectric response of layered composite materials. However, our efforts were preceded by a number of works using similar methods that helped to guide our investigations.

Since many DFT methods exist it is difficult to make ‘apples-to-apples’ comparisons, hence the need for systematic studies of the common explosives. The first group to calculate the THz spectra and molecular properties of various explosives with modern DFT methods was that of T.M. Korter at Syracuse University (Allis et al., 2006a, 2006b, 2008). This was not the earliest work on the subject but is rather cited as the most similar in method to our approach. Earlier work exists on many individual molecular explosives properties and their structure, e.g., for HMX (Häußler et al., 2002; Hooper et al., 2009), for PETN (Burnett et al., 2010) and for RDX (Rice and Chabalowski, 1997). These papers all use DFT methods; however since methods used for exchange and correlation vary, not all are precisely comparable, especially for works prior to ca. 2005. For that reason, the data in Allis et al. (2006a, 2006b, 2008) are our primary reference.

Our own group, which was formed as collaboration between the US Naval Research Laboratory and the US Naval Academy, along with George Mason University and Hunter College, has published five papers so far. For  $\beta$ -HMX, the data first reported in Shabaev et al. (2011b) in *Applied Spectroscopy*, is summarised here. However, the information in that work is updated in the present work with a new prototype simulation. For an estimation of ground-state properties and dielectric response of another high explosive PETN, see Shabaev et al. (2011c) in *Proceedings of SPIE*. For a comparison of the THz dielectric properties of RDX and TNT for the design of detectors, see Shabaev et al. (2011a) in *Journal of Materials Engineering and Performance*. For ‘apples-to-apples’ comparison of the dielectric response of HMX, PETN, RDX and TNT at THz frequencies, see Huang et al. (2012a) in *Journal of Materials Engineering and Performance*. For the THz dielectric properties of clusters representing crystals of PETN and TNT, see Huang et al. (2012b) in *Journal of Materials Engineering and Performance*.

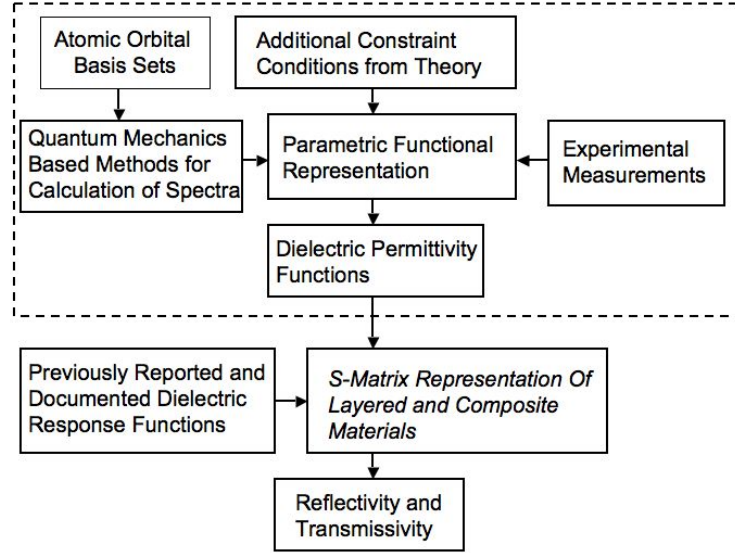
The comparison of many methods for obtaining spectra, both experimentally and computationally determined, is important in the light of the commentary in Kemp (2011) regarding the distinguishability of various explosives’ spectroscopic signatures from ordinary, everyday materials. The success of the proposed methods to probe matter with THz radiation will only be achieved by extreme accuracy in both the models for response and absorption, and the detector’s sensitivity in many environments.

### 3 General simulation framework

A schematic representation of the general framework for numerical simulation of IED response is shown in Figure 1. It should be emphasised that this represents an initial construction, and that the general framework shown in Figure 1 is subject to subsequent refinement and modifications with respect to the paths of input and output from the different model components comprising the framework. The conventional approach, which is to use a database of dielectric response functions associated with different types of materials, is a subset of the paths shown in Figure 1 without the theoretical input. In addition, it should be noted that this simulation framework assumes that data generated from DFT is of comparable accuracy to data obtained from experimental (laboratory

measurement) for the purpose of constructing permittivity function for use in S-matrix based simulations.

**Figure 1** General framework for numerical simulation of IED detection



## 4 Description of component models

### 4.1 S-matrix representation of layered composite system

The central component of the general simulation framework, to which the outputs of all the other component models are inputs, is that of an S-matrix representation of multilayered composites, where each layer of the system is characterised by an average thickness and effective electric permittivity function (Landau et al., 1984; Roeser and Mazur, 2005). The outputs of this central component are the reflectivity and transmissivity as a function of frequency, angle  $\phi$ , and polarisation of the incident electromagnetic wave. The formulation of the S-matrix representation is defined by the following system of equations.

The reflectivity  $R$  and transmissivity  $T$  functions are given by

$$R = \frac{S_{21}}{S_{11}} \text{ and } T = \frac{1}{S_{11}} \quad (1)$$

respectively, where the S-matrix elements  $S_{ii}$  are define by the matrix relation

$$[S] = \begin{pmatrix} S_{11} & S_{12} \\ S_{21} & S_{22} \end{pmatrix} = \left( \prod_{j=1}^m [M_j] \right) [I_{m(m+1)}], \quad (2)$$

where  $[M_j] = [I_{(j-1)j}][L_j]$  and  $m$  is the total number of layers. The matrix  $[I_{ab}]$  is defined by the matrix relation

$$[I_{ab}] = \frac{1}{t_{ab}} \begin{pmatrix} 1 & r_{ab} \\ r_{ab} & 1 \end{pmatrix}, \quad (3)$$

where

$$r_{ab} = \frac{\varepsilon_b S_a - \varepsilon_a S_b}{\varepsilon_b S_a + \varepsilon_a S_b} \text{ and } t_{ab} = \frac{2\varepsilon_b S_a}{S_a + S_b} \quad (4)$$

for a  $p$ -polarised incident wave, and

$$r_{ab} = \frac{S_a - S_b}{S_a + S_b} \text{ and } t_{ab} = \frac{2S_a}{\varepsilon_b S_a + \varepsilon_a S_b} \quad (5)$$

for an  $s$ -polarised incident wave, where equation (5)

$$S_a = (\varepsilon_a - \varepsilon_a \sin^2 \phi)^{1/2} \text{ and } S_b = (\varepsilon_b - \varepsilon_a \sin^2 \phi)^{1/2} \quad (6)$$

and  $\varepsilon_a$  and  $\varepsilon_b$  are the permittivity functions for layers 'a' and 'b', respectively. The matrix  $[L_j]$  is defined by the matrix relation

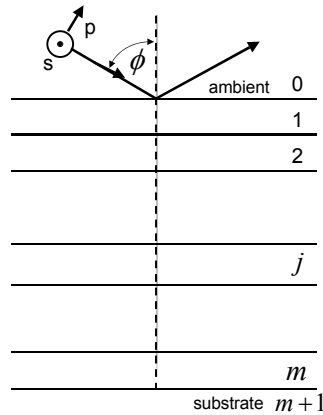
$$[L_j] = \begin{pmatrix} X_j^{1/2} & 0 \\ 0 & 1/X_j^{1/2} \end{pmatrix}, \quad (7)$$

where

$$X_j = \exp \left[ -2\pi i \left( \frac{d_j}{D_j(\phi)} \right) \right], D_j(\phi) = \frac{1}{2\nu} \frac{1}{S_j}, S_j = (\varepsilon_j - \varepsilon_0 \sin^2 \phi)^{1/2} \quad (8)$$

and  $\nu = 1/\lambda$  where  $\lambda$  is the wave length,  $\varepsilon_j$  and  $\varepsilon_{j-1}$  are the permittivity functions for layers ' $j$ ' and ' $j-1$ ', respectively. The quantity  $d_j$  is the thickness of layer  $j$ . The layer indexing used in equations (1) through (8) is defined with reference to Figure 2. A computer program for numerical implementation of equations (1) through (8) is given in Shabaev et al. (2010).

**Figure 2** Schematic representation of layer indexing used in equations (1) through (8)



#### 4.2 Dielectric permittivity functions

The set of permittivity functions that are associated with the different layers comprising the layered composite system represent the primary input to the S-matrix model component. These functions are to be constructed in principle for a given material according to a 'best fit' of available information associated with the electromagnetic response of that material. For a given material this information consists of data obtained from both experimental measurements, e.g., reflectivity and absorption measurements, and numerical simulations based on basic principles, e.g., DFT calculations. It is important to note that the best fit to the electromagnetic response of a given material will depend on the specific response signature characteristics of that material. Accordingly, from the perspective of numerical simulation, a best fit can be in the form of a tabulated functional dependence, as well as parametric representations using analytical functions.

There are specific materials that are typically present in the ambient environment associated with IED detection as well as the detection of other types of materials, e.g., water and water vapour. Accordingly, the electromagnetic response characteristics of these materials have been experimentally investigated by many groups and the results are available. It follows that the permittivity functions of these materials should represent a permanent 'data base' component of the general simulation framework. Examples of the measurement of absorption coefficients of selected explosives that are covered by different types of materials (plastic, cotton, leather and water) are given in Chen et al. (2007).

#### 4.3 Density functional theory

The application of DFT and related methodologies for the determination of electromagnetic response characteristics is important for the analysis of parameter sensitivity. That is to say, many characteristics of the electromagnetic response of a given material may not be detectable, or in general, not relevant for detection. Accordingly, sensitivity analyses concerning the electromagnetic response of layered composite systems can adopt the results of simulations using DFT, and related methodologies, to provide realistic limits on detectability that are independent of a specific system design for IED detection. In addition, analyses of parameter sensitivity based on atomistic response characteristics of a given material, obtained by DFT, provide for constraints on the fitting of experimental measurements for the construction of permittivity functions. It follows that, within the context of parameter sensitivity analysis, data obtained by means of DFT represents a useful complement to data that has been obtained by means of experimental measurements.

The NRLMOL software can be used to compute an approximation of the IR absorption spectrum of a molecule (Pederson and Jackson, 1990; Jackson and Pederson, 1990; Briley et al., 1998; Porezag and Pederson, 1996, 1999; Pederson et al., 2000; Jackson et al., 1997). NRLMOL uses DFT to compute the ground state electronic structure in the Born-Oppenheimer approximation using Kohn-Sham DFT (Kohn and Sham, 1965). NRLMOL uses a Gaussian orbital basis to describe the electronic wavefunctions and density, with numerical integration that is nearly exact to machine precision. For a given set of nuclear positions, the calculation directly gives the electronic charge density of the molecule, the total energy  $E$ , and the forces on each atom.

$$F_{\alpha}^i = \frac{\partial E}{\partial r_{\alpha}^i} \quad (9)$$

where  $r_{\alpha}^i$  is the  $a$  Cartesian component of the position of atom  $i$ , and  $F_{\alpha}^i$  is the corresponding force. The dipole moment of the molecule is easily computed from the combined (nuclear and electronic) charge density.

To compute the minimum energy atomic configuration, NRLMOL uses the conjugate-gradient algorithm (Hager and Zhang, 2006). The vibrational spectrum depends on the atomic mass matrix  $M_{i\alpha j\beta} = \delta_{ij}\delta_{\alpha\beta}m_i$  where  $m_i$  is the mass of atom  $i$ , and on the energy second derivative matrix

$$D_{i\alpha j\beta} = \frac{\partial^2 E}{\partial r_{\alpha}^i \partial r_{\beta}^j}, \quad (10)$$

through the eigenproblem

$$\sum_{j\beta} (D_{i\alpha j\beta} - \varepsilon_n M_{i\alpha j\beta}) X_{j\beta}^{(n)} = 0. \quad (11a)$$

The generalised eigenvalues  $\varepsilon_n$  are the squares of the angular vibration frequencies  $\omega_n = 2\pi c\nu_n$ , and the eigenvectors  $X_{j\beta}^{(n)}$  give the corresponding atomic displacements:

$$\Delta r_{j\beta} = \sum_n Q_n \cdot X_{j\beta}^{(n)}, \quad (11b)$$

where  $Q_n$  is the normal mode coordinate. The eigenvectors are normalised according to the condition

$$\sum_{i\alpha, j\beta} X_{i\alpha}^{(m)} M_{i\alpha j\beta} X_{j\beta}^{(n)} = \delta_{mn}. \quad (11c)$$

NRLMOL computes the energy second derivatives equation (10) by finite differences, computing the forces for displacement perturbations of each atom along each Cartesian direction. The first derivatives of the dipole moment with respect to atomic positions  $\partial \vec{\mu} / \partial r_{\alpha}^i$  are also computed at the same time. Each vibrational eigenmode leads to one peak in the absorption spectrum, at a frequency equal to the mode's eigen frequency. It is significant to note, however, that the finite-difference energy second derivatives represent an approximation of the exact second derivatives and a correction that reduces the associated error of this approximation is obtained by directly recomputing the second derivatives of the energy with respect to the eigenvectors displacements.

The absorption intensity corresponding to a particular eigenmode for a single molecule is given by

$$I_n = \frac{\pi}{3c} \left| \frac{d\vec{\mu}}{dQ_n} \right|^2, \quad (12)$$

where  $c$  is the speed of light in a vacuum, and

$$\frac{d\vec{\mu}}{dQ_n} = \sum_{i\alpha} \frac{\partial \vec{\mu}}{\partial r_{\alpha}^i} X_{i\alpha}^{(n)}. \quad (13)$$

The intensity equation (12) must then be multiplied by the number density of molecules to give an absorption strength. It follows that the absorption spectrum calculated by NRLMOL is a sum of delta functions whose positions and magnitudes correspond to the vibrational frequencies and absorption intensities, respectively. In principle, however, these spectral components must be broadened and shifted to account for anharmonic effects, such as finite mode lifetimes and inter-mode couplings.

#### 4.4 Experimental measurements

The information that is adopted for the construction of permittivity functions is obtained primarily from experimental measurements of electromagnetic response characteristics. Some major issues associated with these constructions are that such experimental measurements typically involve bulk material response characteristics as well as measurement errors due to sample surface preparations and artefacts due to ambient environmental influences. These issues are significant in that the permittivity functions adopted as input are typically assumed as being associated with ‘pure’ materials as well as representative of response characteristics on a small scale that may be typical of thin-film type layers. As in the case of response characteristics that are determined via atomistic calculations, certain response features associated with response characteristics determined by experimental measurement may not be relevant for the simulation of IED detection. That is to say, certain features such as the locations and amplitudes of response spectra may be essential for inclusion into model representations, while only a reasonable estimate of the widths may be necessary. It follows that a sensitivity analysis for parameterisations of experimental measurements is as relevant as those associated with theoretical predictions. Such a sensitivity analysis is another application that is achievable in principle using the simulation framework presented here.

### 5 Prototype analysis (THz excitation)

Presented in this section are prototype simulations for demonstrating some aspects of the relationship between the various model components that comprise the general simulation framework. For this simulation, the response of a layer of  $\beta$ -HMX to THz excitation is considered (Hooper et al., 2009; Häußler et al., 2002; Allis, et al., 2006a, 2006b).

The general approach of constructing permittivity functions according to the best fit of available data for given material corresponding to many different types of experimental measurements is not unprecedented and has been typically the dominant approach, e.g., the permittivity function of water. The general simulation framework presented here considers an extension of this approach in that calculations of electromagnetic response based on DFT are also adopted as data for the construction of permittivity functions. The inclusion of this type of information is essential for accessing what spectral response features at the molecular level are actually detectable with respect to a given set of detection parameters. Accordingly, permittivity functions having been constructed using DFT calculations provide a quantitative correlation between macroscopic material response and molecular structure. Within this context, it is not important that the permittivity function be quantitatively accurate for the purpose of being adopted as input for system simulation. Rather, it is important that the permittivity

function be qualitatively accurate in terms of specific dielectric response features for the purpose of sensitivity analysis, which is relevant for the assessment of absolute detectability of different types of molecular structure with respect to a given set of detection parameters. That is to say, permittivity functions that have been determined using DFT can provide a mechanistic interpretation of material response to electromagnetic excitation that could establish the applicability of a given detection methodology for detection of specific molecular characteristics. Within the context of practical application, permittivity functions having been constructed according to the best fit of available data would be ‘correlated’ with those obtained using DFT for the proper interpretation of permittivity-function features. Subsequent to establishment of good correlation between DFT and experiment, DFT calculations can be adopted as constraints for the purpose of constructing permittivity functions, whose features are consistent with molecular level response, for adjustment relative to specific sets of either experimental data or additional molecular level information.

The construction of permittivity functions using DFT calculations involves, however, an aspect that requires serious consideration. This aspect concerns the fact that a specific parametric-function representation must be adopted. This significant aspect of constructing permittivity functions using DFT, and related methodologies, is indicated explicitly in Figure 1. Accordingly, any parametric representation, i.e., parameterisation, adopted for permittivity-function construction must be physically consistent with specific molecular response characteristics, while limiting the inclusion of feature characteristics that tend to mask response signatures that may be potentially detectable.

In principle, parameterisations are of two classes. One class consists of parameterisations that are directly related to molecular response characteristics. This class of parameterisations would include spectral scaling and width coefficients. The other class consists of parameterisations that are purely phenomenological and are structured for optimal and convenient best fits to experimental measurements. A sufficiently general parameterisation of permittivity functions is given by Drude-Lorentz approximation (Roeser and Mazur, 2005)

$$\varepsilon(\nu) = \varepsilon'(\nu) + i\varepsilon''(\nu) = \varepsilon_\infty + \sum_{n=1}^N \frac{\nu_{np}^2}{(\nu_{n0}^2 - \nu^2) - i\gamma_n \nu}, \quad (14)$$

where  $\nu_{n0}$  is the frequency,  $\nu_{np}$  and  $\gamma_n$  are the spectral scaling and width of a resonance contributing to the permittivity function. The permittivity  $\varepsilon_\infty$  is a constant since the dielectric response at high frequencies is substantially detuned from the probe frequency. The real  $\varepsilon_r(\nu)$  and imaginary  $\varepsilon_i(\nu)$  parts of the permittivity function can be written separately as

$$\varepsilon_r(\nu) = \varepsilon_\infty + \sum_{n=1}^N \frac{\nu_{np}^2(\nu_{n0}^2 - \nu^2)}{(\nu_{n0}^2 - \nu^2)^2 + \gamma_n^2 \nu^2}, \quad \varepsilon_i(\nu) = \sum_{n=1}^N \frac{\nu_{np}^2 \gamma_n \nu}{(\nu_{n0}^2 - \nu^2)^2 + \gamma_n^2 \nu^2}. \quad (15)$$

With respect to practical application, the absorption coefficient  $\alpha$  and index of refraction  $n_r$ , given by

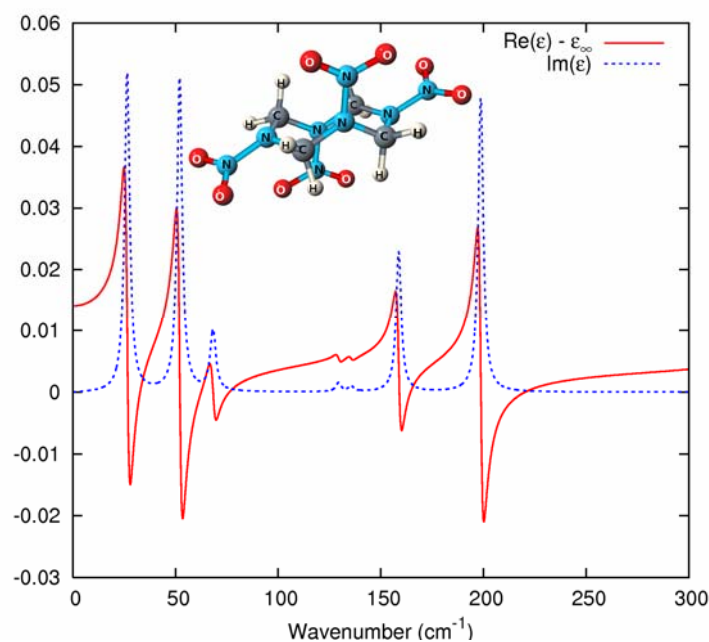
$$\alpha = \frac{4\pi\nu}{\sqrt{2}} \left[ -\varepsilon_r + \sqrt{\varepsilon_r^2 + \varepsilon_i^2} \right]^{1/2} \quad \text{and} \quad n_r = \frac{1}{\sqrt{2}} \left[ \varepsilon_r + \sqrt{\varepsilon_r^2 + \varepsilon_i^2} \right]^{1/2}, \quad (16)$$

respectively, provide direct relationships between calculated quantities obtained by DFT and ‘conveniently measurable’ quantities  $\alpha$  and  $n_r$ .

At this stage it is instructive to present a prototype calculation demonstrating analysis, e.g., interpretation, of permittivity-function features using DFT calculations. Consistent with the prototype simulation presented above, a permittivity function is constructed using DFT calculations for  $\beta$ -HMX response to THz excitation. Figure 3 (inset) shows a general description of the geometry of the  $\beta$ -HMX molecule. The molecular structure was generated by the DFT software NRLMOL for the calculation of a permittivity function using DFT.

In the harmonic approximation, each vibrational-mode frequency corresponds to an oscillator which can be represented by a series of energy levels  $h\nu_n(k + 1/2)$  numbered by  $k = 0, 1, 2, \dots$  with an equal spacing of  $h\nu_n$  on the scale of several THz. Each vibrational frequency is surrounded by a very dense spectrum of rotational modes with the separation between them orders of magnitude lower than a typical frequency of molecular vibrations. The rotational frequencies are on the scale of GHz frequencies, which are not resolved if the THz probe has a relatively broad linewidth.

**Figure 3** Real (solid) and imaginary (dashed) parts of permittivity function of  $\beta$ -HMX molecules with  $\gamma_n = 3 \text{ cm}^{-1}$  and  $\rho = 2.5 \times 10^{19} \text{ cm}^{-3}$  for frequencies within THz range (see online version for colours)



Notes: Inset: molecular structure of  $\beta$ -HMX used for DFT calculations of spectral response

The Drude-Lorentz permittivity function provides an adequate approximation for relatively low concentrations of molecules represented by oscillators that independently scatter THz waves. The resonance frequencies and spectral scalings are acquired from the vibrational analysis supplied by NRLMOL. The frequencies are given by the solutions of

equation (11) where  $v_{n0} = v_n$  and the scalings are estimated from the vibrational intensities  $I_n$  according to

$$v_{np}^2 = \rho \cdot \frac{3}{\pi^2 c} I_n, \quad (17)$$

where  $\rho$  is the number of molecules per unit volume. Figure 3 shows the absorption coefficient and index of refraction corresponding to the density  $\rho = 2.5 \times 10^{19} \text{ cm}^{-3}$ , and all width parameters  $\gamma_n = 3 \text{ cm}^{-1}$ , as defined according to the parameterised permittivity functions given by equations (14) and (15). This density is that of a highly dilute system of molecules within an inert environment, i.e., two orders of magnitude less than that characteristic of a solid. This type of dilute system of explosive molecules would be associated, in principle, with detection scenarios considering vapours that could be released from bulk systems within a bounded region.

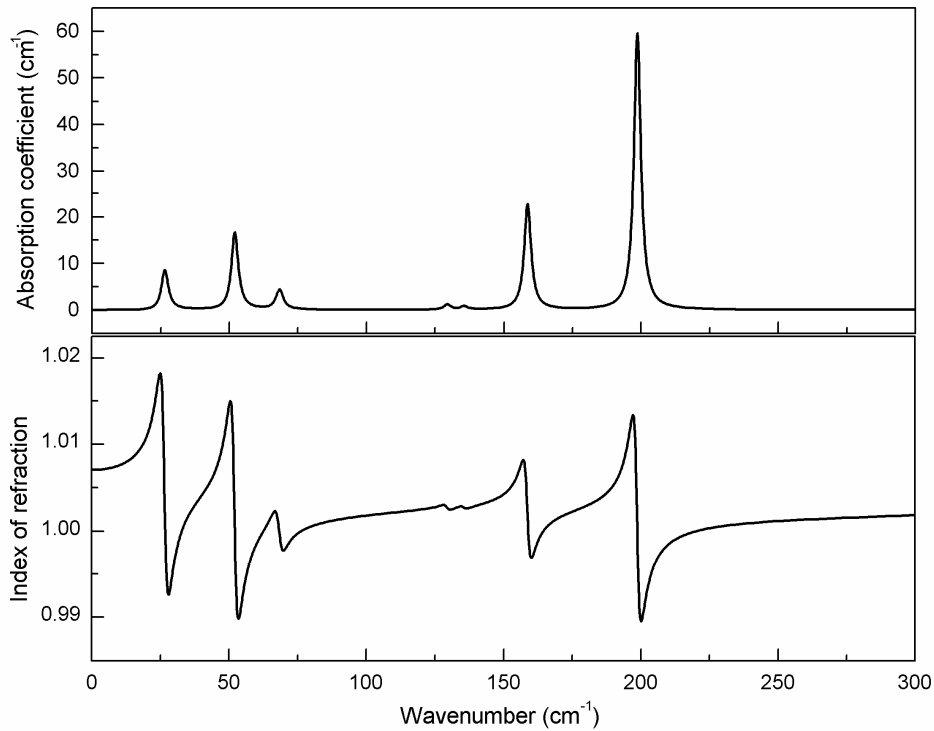
Proceeding with our prototypes analysis, a permittivity function is constructed using the DFT calculations of NRLMOL and the parametric-function representation defined by equations (14) and (15). Accordingly, shown in Figure 3 are the real and imaginary parts of a permittivity function corresponding to the electromagnetic response of  $\beta$ -HMX molecules to excitation within the THz range of frequencies where the widths of the molecular resonances and the density of molecules are chosen at the following values:  $\gamma_n = 3 \text{ cm}^{-1}$  and  $\rho = 2.5 \times 10^{19} \text{ cm}^{-3}$ .

As indicated previously, the parameterisations applied to DFT calculations will in general consist of two classes of parameterisations, i.e., one consistent with basic theory and the other consistent with optimal and convenient best fitting of experimental measurements. Accordingly, one class of parameterisation defines a problem requiring further analysis in terms of basic theory (Wilson et al., 1955; Rice and Chabalowski, 1997; Allis and Korter, 2006), while the other class defines a problem requiring analysis in terms of inverse-problem and parameter-optimisation methodologies (Lambrakos et al., 2001). In principle, the absorption coefficients represent two types of information for input into the simulation framework. The absorption coefficient shown in Figure 4, contains detailed information concerning the enumeration of modes, as well as molecular level response structure obtained by DFT (using NRLMOL). Figure 4 shows a parametric-function fit, using equations (16), to an absorption coefficient for a relatively low density of  $\beta$ -HMX molecules. This function, however, which is the result of a ‘computational experiment’, is characterised by errors associated with numerical artefacts and assumptions concerning bulk structure and micro-to-macro scaling. Accordingly, we note that DFT calculations provide a quantitative initial estimate of molecular response to electromagnetic excitation, which is adaptable to convenient parameterisation for subsequent adjustment with respect to additional information (see Figure 1). The experimentally measured absorption coefficient shown in Hooper et al. (2009) presents another example of a dielectric response function of  $\beta$ -HMX that contains information concerning the bulk response of the material where molecules form a high-density crystal. This function, however, which is the result of a ‘laboratory experiment’, is characterised by errors associated with sample preparation, measurement environment, (e.g., ambient atmosphere and surface contaminants) and resolution characteristic of the detector system.

Shown in Figure 5 are reflectivity functions corresponding to S-polarisation of the incident wave. For this calculation, the layered system consists of a layer of  $\beta$ -HMX

molecules uniformly distributed upon a gold substrate, which is represented by the permittivity function equation (14) for a single term, where  $\epsilon_\infty = 1$ , a zero frequency value  $\nu_0 = 0$ , and a width  $\gamma_0$  due to the finite conductivity of gold. The scaling factor  $\nu_{0p} = 7.27 \times 10^4 \text{ cm}^{-1}$  and width  $\gamma_0 = 2.17 \times 10^2 \text{ cm}^{-1}$  can be obtained from fits to experimental data [see Ordal et al. (1983) and Linden et al. (2004)]. In the THz range, the gold substrate acts as a non-selective mirror, since its permittivity, although varying with frequency, remains large in both real and imaginary parts. It is important to note, however, that for this calculation the layer of  $\beta$ -HMX is of sufficient thickness that contributions due to the substrate can be neglected (see Figure 2). A low transmission through an optically dense absorbing layer reduces the output below the level of detectability. To be noted is that the amplitude of the reflected wave depends on the difference between the permittivity functions of the two adjacent materials forming the interface, and therefore the detection method can be based on measurement of reflected fields in cases where the transmissivity is relatively low (Federici et al., 2005).

**Figure 4** Absorption coefficient (upper) and index of refraction (lower) for  $\beta$ -HMX molecules calculated by DFT for THz range of frequencies corresponding to adjustable parameters  $\gamma_n = 3 \text{ cm}^{-1}$  and  $\rho = 2.5 \times 10^{19} \text{ cm}^{-3}$

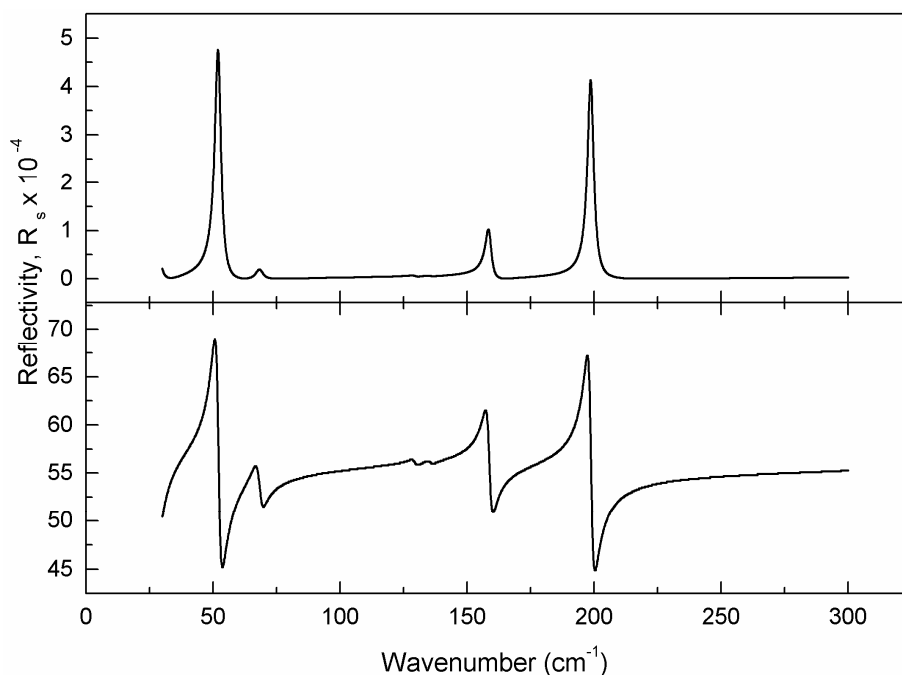


For the optically thick layer of molecules, the reflectivity varies rapidly near the resonances. These sharp features appear in the form of peaks (Figure 5a) or rapidly varying non-monotonic trends (Figure 5b), depending on the high frequency permittivity  $\epsilon_\infty$  within the range of detection frequencies, where it is assumed that only  $\beta$ -HMX

molecules provide the electromagnetic resonances in this system. The reflectivity functions shown in Figure 5 can provide, in principle, a starting point for studies concerning absolute bounds on the detectability of  $\beta$ -HMX molecules under different environmental conditions (i.e., surface layers and ambient environment) and detection scenarios.

An example of the analysis of bounds on detectability is as follows. This analysis considers a detection scenario that includes the use of a gold substrate in combination with relatively thin layers of  $\beta$ -HMX. This hypothetical detection scenario is characteristic of those that would be associated with fibre-optics or waveguide type detection systems. The relatively small thickness of the layers relative to the wavelengths of the incident electromagnetic field makes useful the application of signature enhancement operations, i.e., bin averaging of spectral features. These operations are necessary in that the response of the modelled layer system includes oscillatory structure that is associated with the ideal nature of the interfaces between the layer of  $\beta$ -HMX and its environment.

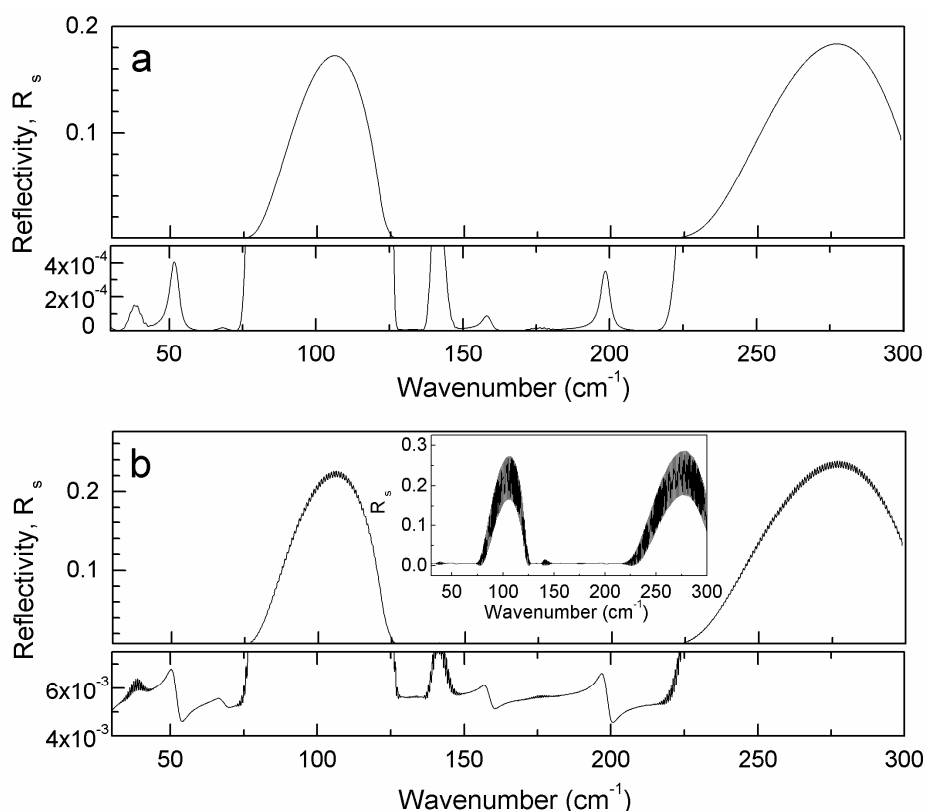
**Figure 5** Reflectivity function  $R_s$  of air- $\beta$ -HMX (200 cm) – gold system for optically thick (200 cm) layer of  $\beta$ -HMX molecules for  $\epsilon_\infty = 1$  (upper) and with  $\epsilon_\infty = 1.2$  (lower)



The effect of scattering at the  $\beta$ -HMX – gold interface is illustrated by Figure 6. The absorption and scattering are rapidly varying functions near the frequencies of molecular resonances. The scattering at the interface with the ambient layer provides detectable features in the reflectivity of an optically dense absorbing layer. For a layer with a relatively low optical density, the absorption is substantially higher only near the resonances where the reflectivity is suppressed compared to a high reflectivity of the interface at the gold substrate. The molecular resonances appear in the form of dips of the

reflectivity function. The reflectivity depends exponentially on the absorption, which changes with frequency according to Figure 3. For a 10 cm layer of  $\beta$ -HMX molecules, this results in orders of magnitude variations in reflectivity with the frequency.

**Figure 6** Reflectivity function  $R_s$  for a 10 cm thick layer of  $\beta$ -HMX molecules ( $\gamma_n = 3 \text{ cm}^{-1}$  and  $\rho = 2.5 \times 10^{19} \text{ cm}^{-3}$ ) below an ambient air environment and above a gold substrate: (a)  $\epsilon_\infty = 1$ , (b)  $\epsilon_\infty = 1.2$  (hypothesised value) with frequency binning (bin size =  $2.4 \text{ cm}^{-1}$ ) for smoothing of rapid oscillations (inset) due to multiple reflections at interfaces

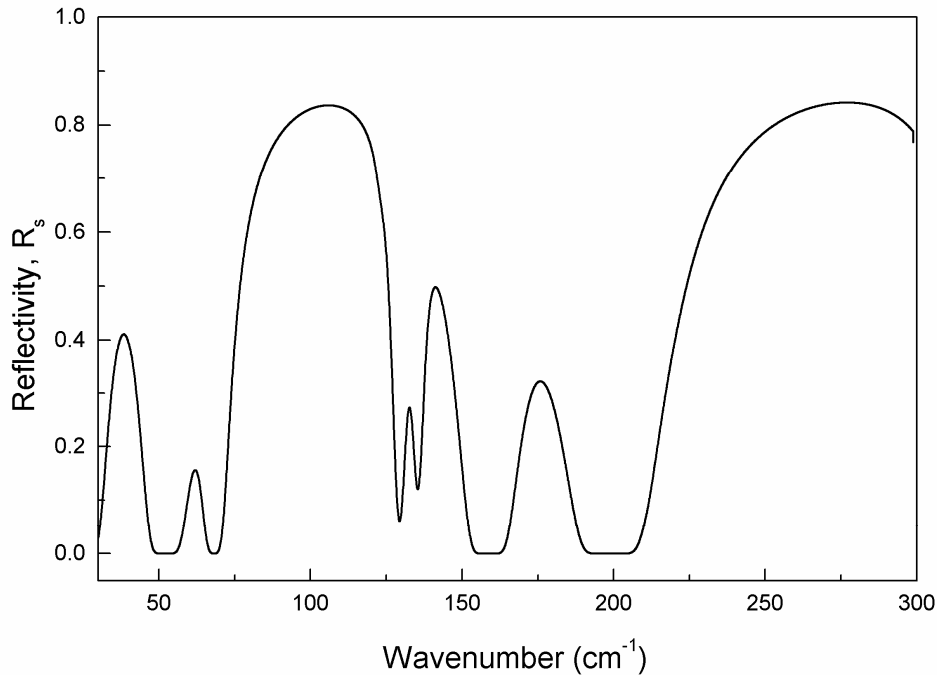


In the range of high transparency between the resonances, the wave can experience multiple reflections from two interfaces on both sides of the layer containing the  $\beta$ -HMX molecules. Far away from the resonances, the reflectivity depends on the difference between the high frequency permittivity  $\epsilon_\infty$  of the  $\beta$ -HMX layer and the permittivity function of the adjacent material, i.e., the gold or air. The reflection from the gold interface is always strong due to the very large permittivity of the metal. The reflection from the air interface substantially varies with  $\epsilon_\infty$ . For  $\epsilon_\infty = 1$  (e.g., air), the reflection between the molecular resonances is negligible. Interestingly, for medium having  $\epsilon_\infty = 1.2$ , for example, the reflection between the resonant peaks is relatively strong owing to oscillations due to multiple reflections. The oscillations are obscured by variation of the frequency or the incident angle. Figure 6b shows the reflectivity after bin averaging,

where bins are of size  $2.4 \text{ cm}^{-1}$ . The reflectivity without binning is shown in the inset. In this detection scenario the detectability of a specific signature feature associated with the THz response spectrum of  $\beta$ -HMX is examined. This feature is associated with a window of relative transparency  $\beta$ -HMX within the range of wavenumbers  $75\text{--}140 \text{ cm}^{-1}$  and  $225\text{--}300 \text{ cm}^{-1}$ . The transparency is low outside of this range, where the reflectivity is determined by the scattering at the air- $\beta$ -HMX interface and the spectra shown in Figure 6a and Figure 6b are those corresponding to the optically thick layer shown in Figure 5.

As the optical thickness decreases, the signature of the molecular resonances becomes more developed in the reflectivity spectrum of the air- $\beta$ -HMX – gold system. For a 1 cm thick layer, the spectrum is shown in Figure 7. In this scenario, the detectability primarily depends on the absorption near the resonances, which determine the contrast of the molecular response in the reflectivity function. Obviously, in the limit of small optical thickness, the molecular signatures become less pronounced since the dips near the resonances flatten and the reflectivity approaches 1 for all frequencies. Accordingly the spectrum shown in Figure 7 is typical of one corresponding to a relatively optimal layer thickness for high sensitivity with respect to detection of absorption signatures.

**Figure 7** Reflectivity function  $R_s$  for a 1 cm thick layer of  $\beta$ -HMX molecules ( $\gamma_n = 3 \text{ cm}^{-1}$  and  $\rho = 2.5 \times 10^{19} \text{ cm}^{-3}$ ,  $\epsilon_\infty = 1$ ) below an ambient air environment and above a gold substrate



## 6 Conclusions

The most significant challenges to explosives-detection will continue to be:

- 1 de-convolving the explosive response spectra from the surrounding materials
- 2 penetrating very absorptive media, such as water.

This work addresses the first of these challenges, although it remains necessary to establish correlation with response properties on the molecular level. We have constructed two types of permittivity functions. One type, whose purpose is the simulation of detection scenarios, represents the best fit to available data, which could include both experimental measurements and calculations based on theory. The other type, obtained using DFT, is that of a reasonably optimal parametric representation of molecular-level response characteristics. By careful examination of many more materials under THz irradiation, it is hoped that by using our methodology it will be possible to distinguish the subtle signatures of explosives, even in highly complex chemical environments.

## Acknowledgements

This work was supported by the Office of Naval Research.

## References

- Allis, D.G. and Korter, T.M. (2006) 'Theoretical analysis of the terahertz spectrum of the high explosive PETN', *ChemPhysChem*, Vol. 7, No. 11, pp.2398–2408.
- Allis, D.G., Prokhorova, D.A. and Korter, T.M. (2006a) 'Solid-state modeling of the terahertz spectrum of the high explosive HMX', *The Journal of Physical Chemistry A*, Vol. 110, No. 5, pp.1951–1959.
- Allis, D.G., Prokhorova, D.A., Fedor, A.M. and Korter, T.M. (2006b) 'First principles analysis of the terahertz spectrum of PETN', *Proceedings of SPIE*, Vol. 6212, No. 62120F, doi:10.1117/12.665787, 8p.
- Allis, D.G., Zeitler, J.A., Taday, P.F. and Korter, T.M. (2008) 'Theoretical analysis of the solid-state terahertz spectrum of the high explosive RDX', *Chemical Physics Letters*, Vol. 463, Nos. 1–3, pp.84–89.
- Briley, A., Pederson, M.R., Jackson, K.A., Patton, D.C. and Porezag, D.V. (1998) 'Vibrational frequencies and intensities of small molecules: all-electron, pseudopotential, and mixed-potential methodologies', *Physical Review B*, Vol. 58, No. 4, pp.1786–1793.
- Burnett, A.D., Kendrick, J., Cunningham, J.E., Hargreaves, M.D., Munshi, T., Edwards, H.G.M., Linfield, E.H. and Davies, A.G. (2010) 'Calculation and measurement of terahertz active normal modes in crystalline PETN', *ChemPhysChem*, Vol. 11, No. 2, pp.368–378.
- Chen, J., Chen, Y., Zhao, H., Bastiaans, G.J. and Zhang, X-C. (2007) 'Absorption coefficients of selected explosives and related compounds in the range of 0.1–2.8 THz', *Optics Express*, Vol. 15, No. 19, pp.12060–12067.
- Federici, J.F., Schulkin, B., Huang, F., Gary, D., Barat, R., Oliveira, F. and Zimdars, D. (2005) 'THz imaging and sensing for security applications-explosives, weapons and drugs', *Semiconductor Science and Technology*, Vol. 20, No. 7, pp.S266–S280.

- Hager, W.W. and Zhang, H. (2006) 'A survey of nonlinear conjugate gradient methods', *Pacific Journal of Optimization*, Vol. 2, No. 1, pp.35–58.
- Häubler, A., Klapötke, T.M., Holl, G. and Kaiser, M. (2002) 'A combined experimental and theoretical study of HMX (Octogen, Octahydro-1,3,5,7-Tetranitro-1,3,5,7-Tetrazocine) in the gas phase', *Propellants, Explosives, Pyrotechnics*, Vol. 27, No. 1, pp.12–15.
- Hohenberg, P. and Kohn, W. (1964) 'Inhomogeneous electron gas', *Physical Review*, Vol. 136, No. 3B, pp.B864–B871.
- Hooper, J., Mitchell, E., Konek, C. and Wilkinson, J. (2009) 'Terahertz optical properties of the high explosive  $\beta$ -HMX', *Chemical Physics Letters*, Vol. 467, Nos. 4–6, pp.309–312.
- Huang, L., Shabaev, A., Lambrakos, S.G., Bernstein, N., Jacobs, V., Finkenstadt, D. and Massa, L. (2012a) 'Dielectric response of high explosives at THz frequencies calculated using density functional theory', *Journal of Materials Engineering and Performance*, Vol. 21, No. 7, pp.1120–1132.
- Huang, L., Shabaev, A., Lambrakos, S.G. and Massa, L. (2012b) 'THz dielectric properties of molecular clusters of PETN and TNT calculated by density functional theory', *Journal of Materials Engineering and Performance*, Vol. 21, No. 8, pp.1620–1636.
- Jackson, K., Pederson, M.R., Porezag, D., Hajnal, Z. and Frauenheim, T. (1997) 'Density-functional-based predictions of Raman and IR spectra for small Si clusters', *Physical Review B*, Vol. 55, No. 4, pp.2549–2555.
- Jackson, K.A. and Pederson, M.R. (1990) 'Accurate forces in a local-orbital approach to the local-density approximation', *Physical Review B*, Vol. 42, No. 6, pp.3276–3281.
- Jaruwatanadilok, S., Kuga, Y., Ishimaru, A. and Thorsos, E. (2006) 'An electromagnetic model for detecting explosives under obscuring layers', *Seventh International Symposium on Technology and the Mine Problem*, 2–4 May, pp.1–10, Monterey, CA
- Jones, R.O. and Gunnarson, O. (1989) 'The density functional formalism, its applications and prospects', *Reviews of Modern Physics*, Vol. 61, No. 3, pp.689–746.
- Kemp, M.C. (2011) 'Explosives detection by terahertz spectroscopy – a bridge too far?', *IEEE Transactions on Terahertz Science and Technology*, Vol. 1, No. 1, pp.282–292.
- Kohn, W. and Sham, L.J. (1965) 'Self-consistent equations including exchange and correlation effects', *Physical Review*, Vol. 140, No. 4A, pp.A1133–A1138.
- Lambrakos, S.G., Moore, P.G., Loschialpo, P. and Smith, D. (2001) 'Estimates of optical parameters based on mixing rules extending over a wide range of wavelengths', *Applied Spectroscopy*, Vol. 55, No. 5, pp.584–590.
- Landau, L.D., Pitaevskii, L.P. and Lifshitz, E.M. (1984) *Electrodynamics of Continuous Media*, 2nd ed., Vol. 8 (*Course of Theoretical Physics*), Elsevier Butterworth-Heinemann, Oxford-Burlington.
- Linden, S., Enkrich, C., Wegener, M., Zhou, J., Koschny, T. and Soukoulis, C.M. (2004) 'Magnetic response of metamaterials at 100 terahertz', *Science*, Vol. 306, No. 5700, pp.1351–1353.
- Ordal, M.A., Long, L.L., Bell, R.J., Bell, S.E., Bell, R.R., Alexander, R.W. Jr. and Ward, C.A. (1983) 'Optical properties of the metals Al, Co, Cu, Au, Fe, Pb, Ni, Pd, Pt, Ag, Ti, and W in the infrared and far infrared', *Applied Optics*, Vol. 22, No. 7, pp.1099–1119.
- Pederson, M.R. and Jackson, K.A. (1990) 'Variational mesh for quantum-mechanical simulations', *Physical Review B*, Vol. 41, No. 11, pp.7453–7461.
- Pederson, M.R., Porezag, D.V., Kortus, J. and Patton, D.C. (2000) 'Strategies for massively parallel local-orbital-based electronic structure methods', *Physica Status Solidi (B)*, Vol. 217, No. 1, pp.197–218.
- Porezag, D.V. and Pederson, M.R. (1996) 'Infrared intensities and Raman-scattering activities within density-functional theory', *Physical Review B*, Vol. 54, No. 11, pp.7830–7836.
- Porezag, D.V. and Pederson, M.R. (1999) 'Optimization of Gaussian basis sets for density-functional calculations', *Physical Review A*, Vol. 60, No. 4, pp.2840–2847.

- Rice, B.M. and Chabalowski, C.F. (1997) 'Ab initio and nonlocal density functional study of 1,3,5-trinitro-s-triazine (RDX) conformers', *The Journal of Physical Chemistry*, Vol. 101, No. 46, pp.8720–8726.
- Roeser, C.A.D. and Mazur, E. (2005) 'Light-matter interactions on femtosecond time scale', in B. Di Bartolo and O. Forte (Eds.): *Frontiers of Optical Spectroscopy* NATO Science Series, Vol. 168, No. 1, pp.29–54, Kluwer Academic Publishers, Dordrecht – Norwell.
- Shabaev, A., Lambrakos, S.G., Bernstein, N., Jacobs, V. and Finkenstadt, D. (2010) 'Initial construction of a general framework for numerical simulation of IED detection and remote activation scenarios', *Naval Research Laboratory Memorandum Report*, Naval Research Laboratory, Washington, DC, NRL/MR/6390-10-9260.
- Shabaev, A., Lambrakos, S.G., Bernstein, N., Jacobs, V. and Finkenstadt, D. (2011a) 'THz dielectric properties of high explosives calculated by density functional theory for the design of detectors', *Journal of Materials Engineering and Performance*, Vol. 20, No. 9, pp.1536–1543.
- Shabaev, A., Lambrakos, S.G., Bernstein, N., Jacobs, V.L. and Finkenstadt, D. (2011b) 'A general framework for numerical simulation of improvised explosive device (IED)-detection scenarios using density functional theory (DFT) and terahertz (THz) spectra', *Applied Spectroscopy*, Vol. 65, No. 4, pp.409–416.
- Shabaev, A., Lambrakos, S.G., Bernstein, N., Jacobs, V.L. and Finkenstadt, D. (2011c) 'Ground state resonance structure calculated by density functional theory for estimating the dielectric response of the high explosive PETN', *Proceedings of SPIE*, Vol. 8023, No. 80230W, doi:10.1117/12.883279, 8pp.
- Wilson, E.B., Decius, J.C. and Cross, P.C. (1955) *Molecular Vibrations*, McGraw-Hill, New York.